New Journal of Physics
The open-access journal for physics

Ferromagnetic semiconductors and the role of disorder

B W Wessels
Materials Research Center, Northwestern University, Evanston, IL 60208, USA
E-mail: b-wessels@northwestern.edu

New Journal of Physics **10** (2008) 055008 (17pp)
Received 11 January 2008
Published 23 May 2008
Online at http://www.njp.org/
doi:10.1088/1367-2630/10/5/055008

Abstract. In this paper, we report on the role of short-range disorder in stabilizing ferromagnetism in transition metal-doped compound semiconductors. While both theory and experiment have centered on dilute magnetic semiconductors where the magnetic ions substitute randomly for cation sites, there is increasing evidence that correlated substitution needs to be considered. Evidence of correlated substitution comes from structural analysis (extended x-ray absorption fine structure (EXAFS)), magnetic property and recent magneto-optical property measurements as well as theory. Furthermore, there is growing theoretical and experimental support that ferromagnetic semiconductors with Curie temperatures well above room temperature can be formed through correlated substitution. Future materials research will be well served by identification and examination of semiconductor systems that favor short-range ordering of magnetic constituents.

Contents

1367-2630/08/055008+17$30.00

1. Introduction

The ability to synthesize materials that combine both semiconductivity and strong magnetism has been a long sought after goal for materials physics. The potential of using spin of electrons, rather than charge for storing, transmitting and processing information has led to widespread interest in spin effects in semiconductors [1, 2]. Of particular interest are the dilute magnetic semiconductor (DMS) compounds (notably II–VI and III–V semiconductors) where a fraction of the cations are replaced by transition metal ions. More than 25 years ago, it was shown that alloying transition metals with II–VI compound magnetic semiconductors could be realized [3]. These compounds were, however, antiferromagnetic. Some 10 years later, the IBM group showed that by forming III–V alloys containing manganese by molecular beam epitaxy (MBE), ferromagnetism resulted. The Curie temperature was of the order of 30 K [4]. A major breakthrough resulted in 1996 when the synthesis of ferromagnetic GaMnAs with a Curie temperature of 110 K was reported [5]. This set off a worldwide search for semiconductors with a Curie transition above room temperature. Two approaches were taken: optimization of GaMnAs and searching for new classes of magnetic semiconductors.

While significant progress has been made in the improvement of semiconducting and magnetic properties of these compounds, the origin of the ferromagnetism is not well understood. A major question remains as to what type of exchange mechanism stabilizes the ferromagnetic phase, especially in light of the dilute concentration of magnetic ions. Magnetism in non-metals is primarily associated with short-range exchange interactions, but in DMS the distance between magnetic atoms is typically 1–3 nm. The determination of the nature of the exchange interactions that can explain the ferromagnetism is key to the prediction of new combinations of magnetic ions and semiconductor hosts. Of particular interest are mechanisms that stabilize ferromagnetism for semiconductors with dilute concentrations of magnetic ions. Early on a model was proposed for DMS that consisted of two electronic subsystems: one containing delocalized, band electrons and the other consisting of magnetic impurity electrons with localized moments in the 3d shell [6]. The delocalized electrons determine the electrical and optical properties of the ions, whereas the localized magnetic moments are presumed responsible for the magnetic properties. However, strong spin-dependent sp–d exchange interactions occur between the two subsystems.

In II–VI compounds, interactions between the sp–d bands were described by a superexchange mechanism [7]. This leads to stabilization of the antiferromagnetic state as is observed in II–VI DMS. However, the ferromagnetic state observed in III–V InMnAs and GaMnAs cannot be explained by a superexchange model, which only leads to antiferromagnetism in these systems. For III–V DMS compounds, the free carriers must be playing an essential role in stabilizing the observed ferromagnetism. Thus a modified Ruderman, Kittel, Kasuya and Yosida (RKKY) interaction was proposed for stabilizing the ferromagnetism in III–V semiconductors [8].

The RKKY model was widely accepted and often cited for explaining ferromagnetism in these semiconductors. It has been used to predict quantitatively semiconductors that potentially have a Curie temperature in excess of room temperature, a long sought after goal. However, a number of simplifying assumptions were required in order to make calculations tractable including a host-independent exchange energy term. Nevertheless, a number of the electrical, optical and magnetic properties of GaMnAs could be explained within this theoretical framework. This included the observation of ferromagnetism in GaMnAs and the observed dependence of T_c on alloy and carrier concentrations [8]. It was asserted that the quantitative agreement between theory and experiment for the GaMnAs system and the observed Curie temperature dependence on alloy concentration enabled prediction of Curie temperatures for other tetrahedrally coordinated semiconductors, including III–V and II–VI compounds and group IV elements. Calculations indicated that GaMnAs should have a higher T_c than InMnAs, which indeed is the case [8]. In fact it predicted that InMnAs should have a T_c of 35 K, very close to what was experimentally observed for MBE-grown material. As a result, much of the materials and device studies centered on GaMnAs instead of the InMnAs system. Recently however, MBE-grown InMnAs with a Curie temperature of 90 K was reported, 250% greater than that predicted by the RKKY theory [9]! This finding, while remarkable, has been largely ignored by both the theory and experimental communities since the Curie temperature is below 100 K. Nevertheless, it has important ramifications with regard to the accuracy of prior predictions based on the RKKY theory. For example, based on scaling arguments instead of the predicted published value of 110 K for GaMnAs, upon scaling it should be 280 K. Similarly, for GaN, instead of a predicted T_c of 400 K, it should be 1000 K!

Despite early acceptance of the RKKY theory for DMS, there is growing evidence that the approximations taken are too restrictive for quantitative prediction [10, 11]. Bergvist *et al* [12] indicated that a mean field approximation overestimates the critical temperature as compared with that obtained using Monte Carlo simulations and the virtual crystal approximation. Furthermore, Sato *et al* [13] noted that when calculating the Curie temperature in the mean field approximation $k_b T_c = 2/3c \sum J_{0i}$ where c is the magnetic ion concentration and J_{ij} is the effective exchange coupling coefficient between ions i and j, the formula heavily weights nearest-neighbor interaction J_{01}. The mean field value of T_c is mostly determined by J_{01}. *Ab initio* electronic structure calculations using the Korringa–Kohn–Rostoker (KKR) method, however, indicate for higher magnetic ion concentrations that J_{01} is suppressed and even becomes negative. Other longer range exchange terms need to be included.

Accordingly for GaMnN with the Mn ion impurity wavefunction in the gap there is a strong exponential decay of the exchange energy with distance [13]. However, for (GaMn)As, the p–d interactions become important since the impurity level is relatively shallow. Here, the exchange interaction is relatively long-range and extends three lattice constants. For dilute concentrations of magnetic ions, long-range interactions are important due to percolation. Below the percolation threshold, global ferromagnetism cannot be achieved. This effect is not included in the mean-field equation for T_c. The effect of dilution on T_c is only included in the prefactor c. For the Heisenberg model of the near-neighbor interaction the percolation threshold is 20%. For extended exchange interactions, the percolation threshold could be lower. To obtain higher Curie temperatures, longer range interactions or higher concentration are needed.

The situation becomes even more complicated when one considers disordered semiconductor materials where the magnetic ions are not randomly substituted for cation sites. Dietl *et al* [6] limited their calculations to magnetic ions that are randomly distributed on the cation sites. This was generally considered to be the case for alloys deposited by MBE at low temperatures. For the concentrations of interest of 1–10%, ions are, however, not isolated but form near-neighbor pairs and even near-neighbor clusters, even without an attractive interaction energy. This pairing can significantly alter the magnetic properties, including Curie temperature [14]. Nearly 7 years ago, we observed that InMnAs prepared by MOVPE had a Curie temperature of 330 K [15, 16]. Of course there were questions of phase purity, but x-ray diffraction and TEM analysis indicated that the films were nominally phase pure [17]. The high Curie temperature was attributed to formation of atomic-scale magnetic clusters [18].

In this report, the role of short-range disorder in stabilizing ferromagnetism in transition metal-doped semiconductors is considered. There is growing evidence that correlated substitution of magnetic atoms needs to be considered. Evidence of correlated substitution comes from structural analysis (extended x-ray absorption fine structure (EXAFS)), magnetic property and magneto-optical property measurements as well as theory. Furthermore, there is strong theoretical and experimental support that ferromagnetic semiconductors with Curie temperatures well above room temperature can result from correlated substitution. With suitable combinations of magnetic impurity clusters in the DMS, high-T_c material can be achieved. Future materials research will be well served by the identification and examination of semiconductor systems that favor short-range ordering of magnetic constituents in order to obtain materials with high transition temperatures.

2. Models for ferromagnetism

2.1. Limits of the Zener model exchange energy considerations

Ferromagnetic semiconductors with T_c greater than room temperature have been predicted using the RKKY theory. For an RKKY carrier-ion direct exchange, the Hamiltonian is given by $H_{ex} = xN_o\alpha\langle S_{11}\rangle s_{11}$ where s_{11} and $\langle S_{11}\rangle$ are components of the band electron spin and thermodynamic average of the impurity spin, respectively; xN_o is the concentration of magnetic ions and α is the exchange constant for sd electrons. The exchange energy J scales with $xN_o\alpha$ for electrons ($xN_o\beta$ for holes). Initial experimental studies of $Ga_{1-x}Mn_xAs$ alloys showed that T_c, and thus J, scales with Mn concentration up to $x = 0.06$. However, deviation from the linear dependence of T_c on x was noted and attributed to compensation by electrically active defects such as antisites and interstitials [19, 20].

The RKKY model also has predictive capability [8]. Assuming a material-independent exchange constant β of 1.0 eV T_c will scale with N_o, which only depends on host structure and lattice constant. Thus the smaller the lattice constant, the higher the exchange energy and the resultant T_c. Of course the assumption of a constant β is problematic, since it is not a simple linear function of the lattice constant. Indeed, in metals where screening by free carriers is important, there is a non-monotonic dependence of exchange energy on interatomic spacing as seen in figure 1 [21]. While bcc iron is ferromagnetic with a positive exchange energy, fcc iron with a smaller interatomic spacing is antiferromagnetic. Moreover, metallic Mn with a smaller interatomic spacing than bcc iron is also antiferromagnetic. However, for Mn in MnAs and MnSb, the interatomic distances are both larger than metallic Mn and these compounds are ferromagnetic [21]. Thus the calculations by Dietl *et al* based on the simplifying assumption that the exchange energy is inversely proportional to the atomic radius lead to significant overestimates for the Curie temperature for DMS with small lattice constants. This predicts that they will have Curie temperatures well above room temperature. This prediction set off a worldwide search for host semiconductor compounds with small lattice constants such as GaN and ZnO. Conversely, compounds with large lattice constants such as InAs or GaSb were predicted to have a low T_c. While there were numerous reports of a high T_c for doped GaN and ZnO materials, their existence remains controversial. Questions of phase purity and the presence of unintentional magnetic impurities were posed [22].

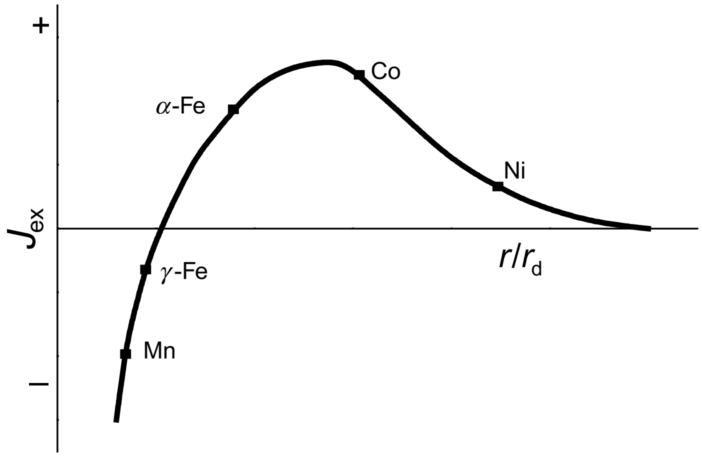

Figure 1. Dependence of exchange energy on interatomic spacing after [21].

There are other reasons why transition metals in wide-gap semiconductors would not yield DMS with high transition temperatures. Transition metals often form deep levels that compensate band carriers [23]. According to Dietl *et al*, T_c depends on carrier concentration; a T_c of 20 K is expected for GaAs with carrier concentrations of less than 10^{19} cm^{-3}. For example in GaN, substitutional Mn forms a deep level of the order of 1.4 eV above the valence band [24]. Thus, addition of Mn leads to semi-insulating material. Of course without free carriers there is no RKKY interaction.

Thus, considering that transition metals form deep levels in wide-gap semiconductors and that the resulting materials are highly resistive, it would indicate that wide-gap semiconductors should have a low T_c. Therefore other hosts should be considered. While transition metal doping of semiconductors has been widely studied, not as much is known about their behavior in narrow-gap semiconductors. Studies have shown that transition metals form shallow levels or even levels resonant with the bands [25]. Thus, high-conductivity materials can result. These narrow-gap semiconductors should be a suitable host that could show carrier-mediated ferromagnetism. Thus, in contrast to earlier predictions, based upon deep level defect formation we propose that narrow-gap hosts are preferred [8]. The closer the level is to the band edge the better. Figure 2 shows the relationship of the Mn acceptor level to the band edge. It can be seen that while Mn is deep in GaN and InP, it is shallow in InAs and resonant in InSb and GaSb [25]. Thus, the last three Mn-doped compounds should be highly conductive as has been shown to be the case for InMnAs.

While their high conductivity makes narrow-gap semiconductors preferable, there are also other considerations that favor these semiconductors. Since T_c depends on free carrier concentration, compensation by oppositely charged defects can lead to a decrease. Indeed the measured hole concentrations in InMnAs and GaMnAs are much lower than the Mn concentration. Native defect formation has been proposed as a factor that limits the conductivity and T_c in GaMnAs [20]. For example in GaMnAs, the As antisite defects have been proposed to limit the hole concentration in MBE material grown at low temperatures. These As antisites are double donors, which compensate the Mn acceptors. Mn interstitial donors have also been indicated as a compensating defect. It is well known that the larger the gap, the greater the energy to be gained by forming compensating defects. Thus, self-compensation of transition

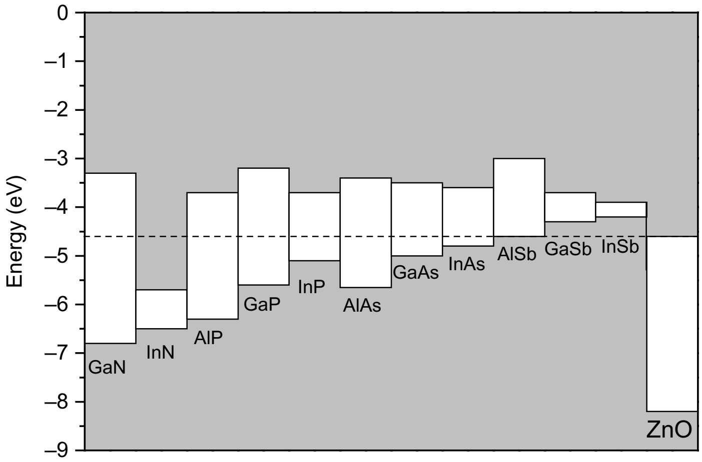

Figure 2. The relationship between the Mn level and the band edge. The dashed line indicates the position of the calculated Mn acceptor level using a vacuum-referred binding energy model after [25].

metal acceptors should be favored in wide-gap semiconductors and is of less importance in narrow-gap materials.

2.2. Role of disorder/cluster formation/precipitates

While the existence of a high-T_c semiconductor stabilized via a carrier-mediated mechanism remains controversial, there is growing evidence that high-T_c semiconductors can be stabilized through other mechanisms. Theoretical calculations using coherent potential approximation (CPA) indicate that disorder can lead to stabilization of ferromagnetism. Bouzerar *et al* [14] developed a quantitative theory for DMS under the assumption that the positions of the substitutional magnetic impurities are correlated. They predicted that room temperature ferromagnetism should be possible in GaMnAs provided that the probability of transition metal pair formation is enhanced. Indeed for completely correlated pair formation, a T_c of 400 K was predicted, whereas for uncorrelated pairs a T_c of 180 K was predicted. The latter is in good agreement with that observed in MBE-grown GaMnAs. Bouzerar *et al* [14] predict that unlike the RKKY theory a threshold should exist for ferromagnetism that depends on concentration. They also noted that according to their calculations GaN should have a T_c a factor of two lower than that of GaAs. Based on their calculations, prescriptions for obtaining a high-temperature ferromagnetic included: working at concentrations of $x = 0.05$–0.10 and preparing samples under conditions where formation of pairs and not precipitates is favored.

Calculations by Kudrnovsky *et al* using CPA considered the stability of DMS. They found that the alloy of GaMnAs is unstable with respect to segregation into related components [26]. They maintain that domains form consisting of two types, regions of low Mn concentration and those with a high Mn concentration. They found that the domain size depends on chemical composition and could be as large as several nanometers. Finally, there was a strong tendency of substitutional Mn atoms with parallel magnetic moments to form.

The calculations of Kudrnovsky *et al* predict that the magnetic components segregate. The recent calculations that spinodal decomposition plays an important role in forming wide-gap ferromagnetic semiconductors further support disorder [27]–[29]. In this case rather large clusters are predicted to form that are rich in magnetic atoms. The clusters, however, are isolated from one another. Low Curie temperatures are presumed to result from missing magnetic percolation paths in the decomposed phase. Whether or not percolation paths form depends on the cluster size, concentration and shape [30]–[32].

For disordered semiconductors, we propose a quasi-chemical model for cluster-mediated ferromagnetism that predicts which alloys would have the highest T_c. It is proposed that T_c for cluster-mediated alloys should tend towards the constituent phase with the highest T_c. For III–V compounds doped with Mn, the end compounds are MnP, MnAs and MnSb, which have T_c values of 280, 320 and 560 K, respectively [21]. T_c increases with increasing interatomic distance. For the host crystal group with In as the primary cation, T_c should increase as follows: InMnN, InMnP, InMnAs and InMnSb. Similarly, for Ga-based alloys, T_c should increase as follows: GaMnN, GaMnP, GaMnAs and GaMnSb. This presumes that Mn-rich alloys with a zinc blende structure can be stabilized. Thus, considering a solid solution between InAs and MnAs, the Mn-rich alloy should have a T_c approaching that of MnAs ($T_c = 320\,\mathrm{K}$), which is consistent with our findings for MOVPE InMnAs.

There is additional theoretical support for such a quasi-chemical approach for predicting high-T_c compounds. Franceschetti *et al* [33] used a cluster expansion formalism to determine, from first principles, configurations that would yield GaMnAs with a T_c above 300 K. Using the formalism they found a configuration with a T_c of 375 K, well above that of a random alloy with the same concentration and 200 K higher than what is experimentally observed. The alloys with the highest T_c, however, were ordered having a $(\mathrm{GaAs})_m/\mathrm{MnAs}$ superlattice structure with layering in the [200] direction. Nevertheless, these calculations indicate that for suitable combinations of magnetic impurity clusters in the DMS, high-T_c material can be achieved.

3. Comparisons to experiments

Models that consider substitutional disorder predict that enhanced T_c should be observed. Since disorder depends on alloy preparation conditions, T_c should also strongly depend on processing conditions. For MBE material deposited at low temperatures, random solid solutions are obtained. Using low temperatures enables the synthesis of alloys with magnetic ion concentrations well in excess of equilibrium solubility. However, III–V ferromagnetic alloys with T_c well below room temperature result. Our work has focused on InMnAs grown by MOVPE prepared at higher temperatures. We have found that InMnAs grown by this technique has a T_c of 330 K [15, 16]. This is counter to the prediction of the RKKY theory of a T_c of 35 K and early experiments on InMnAs grown by MBE. The question of course arises as to why the difference between experiment and theory. Why does the observed T_c depend on the synthesis technique? More puzzling was our finding that T_c was independent of hole concentration p for InMnAs for the composition ranges studied. Furthermore, the carrier concentration was only of the order of $10^{18}\,\mathrm{cm}^{-3}$, which is too low to obtain a high T_c according to the RKKY theory. While second-phase formation was considered as the origin of the high T_c, where the phase is magnetic, extensive x-ray and TEM measurements indicate otherwise [34]. The films were phase pure. We postulated that the increase in T_c was due to disorder resulting from the formation of atomic-scale clusters of Mn in the alloys. The clusters formed upon substitution of Mn on the cation site. While Mn dimers and trimers were originally proposed, larger clusters of Mn_n are believed to form [35].

The model that we used to analyze magnetization and magneto-optical data for the InMnAs is a multisite model whereby the Mn substitutes on In sites as atoms or can form near-neighbor

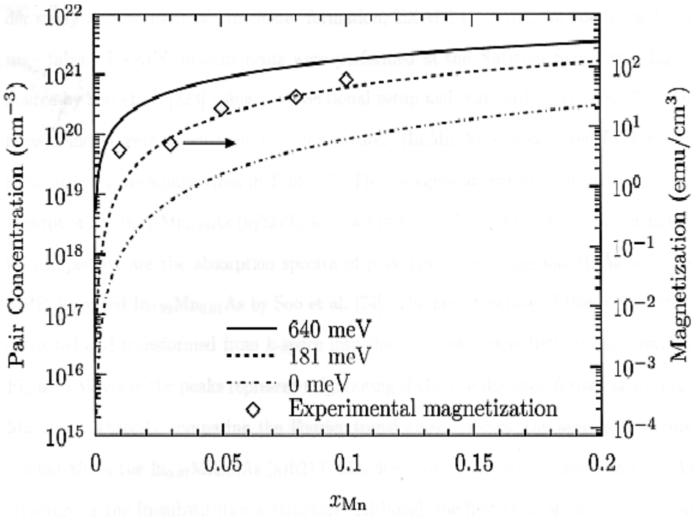

Figure 3. Calculations of the pair concentration as a function of Mn concentration, x. For no interaction can it be seen that for $x = 0.10$ the pair concentration is of the order of 5×10^{19} cm^{-3}. However, with a moderate binding energy of 180 meV, it increases to 5×10^{20} cm^{-3} after [37].

pairs, trimers or other higher order clusters by substituting on near-neighbor cation sites. For analysis we used the solution model for defects in semiconductors described by Reiss [36]. For the case of the simplest cluster, the Mn–Mn pair (dimer) sitting on nearest-neighbor cation sites, the pair concentration P in a dilute solution is given by:

$$\frac{P}{(xN_o - P)^2} = \frac{1}{2N_o} \exp\left(\frac{-E2}{kT}\right), \tag{1}$$

where x is the Mn atomic fraction, N_o is the total cation site density and E_2 is pair formation energy. For InMnAs, N_o is 1.8×10^{22} cm^{-3}. For a low pair concentration, P can be approximated by $P = (1/2)x^2 N_o \exp(-E2/kT)$. Figure 3 shows the initial calculations of the pair concentration as a function of Mn concentration x. For no interaction can it be seen that for $x = 0.10$ the pair concentration is of the order of 5×10^{19} cm^{-3}. However, with a moderate binding energy of 181 meV, the pair concentration increases to 5×10^{20} cm^{-3}. This corresponds to a magnetization of 45 emu cm^{-3} assuming the magnetic moment $\mu = 8\mu_\beta$ per dimer. Also included in the figure are magnetization data for InMnAs grown by MOVPE. Note that the magnetization depends on atomic fraction of Mn, but increases quadratically with x_{Mn} at low concentrations. Preliminary data of Blattner [37] for the measured magnetization indeed show that the magnetization follows the above equation. However, there is an increase in the number of dimers compared to that expected for a simple random solid solution. For $x = 0.1$ if all the atoms were in pairs there should be $xN_o/2$ or 9×10^{20} cm^{-3}. This is to be compared to the 6×10^{20} cm^{-3} we determined for alloys from magnetization data.

Our early experimental EXAFS analysis studies on MOVPE InMnAs support the role disorder plays. EXAFS measurements indicated that Mn substitution was not random but Mn pairs formed when Mn substituted on near-neighbor In sites [38]. This is in contrast to InMnAs grown by low temperature MBE where a random solid solution was observed. EXAFS indicated that the Mn was randomly substituting for In and no clustering was occurring [39].

To determine whether clustering is playing a role in determining the magnetic and magneto-optical properties of the InMnAs alloys grown by MOVPE, we measured and analyzed the magneto-optic Kerr effect (MOKE) for a series of alloys [40]. The magnetic circular dichroism (MCD) is directly related to spin polarization of a semiconductor band [41]. In that study we found that the MOKE signal increased super linearly with Mn composition x. Our previous MCD measurements on this material indicate that sp–d ferromagnetic exchange persists above room temperature up to 330 K [42]. The MCD spectrum over the energy range of 1.6–3.1 eV consists of two prominent features: a broad transition extending from 1.6 to 3.0 eV labeled $|\theta_\mathrm{b}|$, and a negative peak centered between 2.60 and 2.68 eV labeled $|\theta_\mathrm{p}|$. Differences in the temperature dependence of the two features between 273 and 333 K were observed and attributed to the presence of two types of transitions. The broad transition was tentatively ascribed to spin-dependent electronic transitions between the Mn impurity band and conduction band given by the equation [40]:

$$\mathrm{Mn}^{2+} \rightarrow \mathrm{Mn}^{3+} + \mathrm{e}^{-}(\mathrm{CB}). \tag{2}$$

The negative peak at 2.6 eV was attributed to E_1 transitions between spin split valence and conduction bands near the L-critical point (CP). The strong MCD near CPs is a signature of sp–d exchange.

To determine their nature, we investigated the dependence of the MCD on concentration. For Mn-doped III–V and II–VI random alloys, where the majority of Mn are singly substituted on tetrahedrally co-ordinated cation sites, the mean field theory predicts that the magnitude of the dichroism depends linearly on x. However, in *non-random* alloys, Mn preferentially substitutes on nearest-neighbor cation sites to form Mn clusters such as dimers and trimers. The concentration of these clusters has a superlinear dependence on x. From the mean field theory, the magnitude of the MCD should therefore have the same superlinear dependence on concentration. Thus, from the concentration dependence of MCD, the role of Mn atomic-scale clusters and short-range ordering can potentially be determined.

The composition dependence of the dichroic response $|\theta_\mathrm{b}|$ and $|\theta_\mathrm{p}|$ as a function of x assumes that it is proportional to the concentration of the specific cluster species in the material. For example, singly substituted Mn (S), dimers (D), trimers (T), or tetramers (T') will contribute to the dichroism. The dependence on manganese concentration x is given by:

$$\theta_\mathrm{single} = A_1 S = A_1[N_0 x(1-x)^{12}], \tag{3}$$

$$\theta_\mathrm{dimer} = A_2 D = A_2[12N_0 x^2(1-x)^{18}], \tag{4}$$

$$\theta_\mathrm{trimer} = A_3 T = A_3[24N_0 x^3(1-x)^{22}] \tag{5}$$

and

$$\theta_\mathrm{tetramer} = A_4 T' = A_4[48N_0 x^4(1-x)^{26}], \tag{6}$$

where A_n is the proportionality constant relating the concentration of the nth order cluster to the magnitude of the dichroism (units of mdeg cm^3) and N_0 is the nominal cation site concentration. The expressions for S, D, T and T' given in brackets in equations (3)–(5) were previously formulated by Behringer [43]. The spectral response of the MCD (θ) can be described in terms of a superposition of the transitions where $\Theta = \Sigma\theta_n$.

It is important to note that the equations for θ_n do not consider the effect of any thermodynamic tendency to form clusters. Consequently, the magnitudes of the D, T and

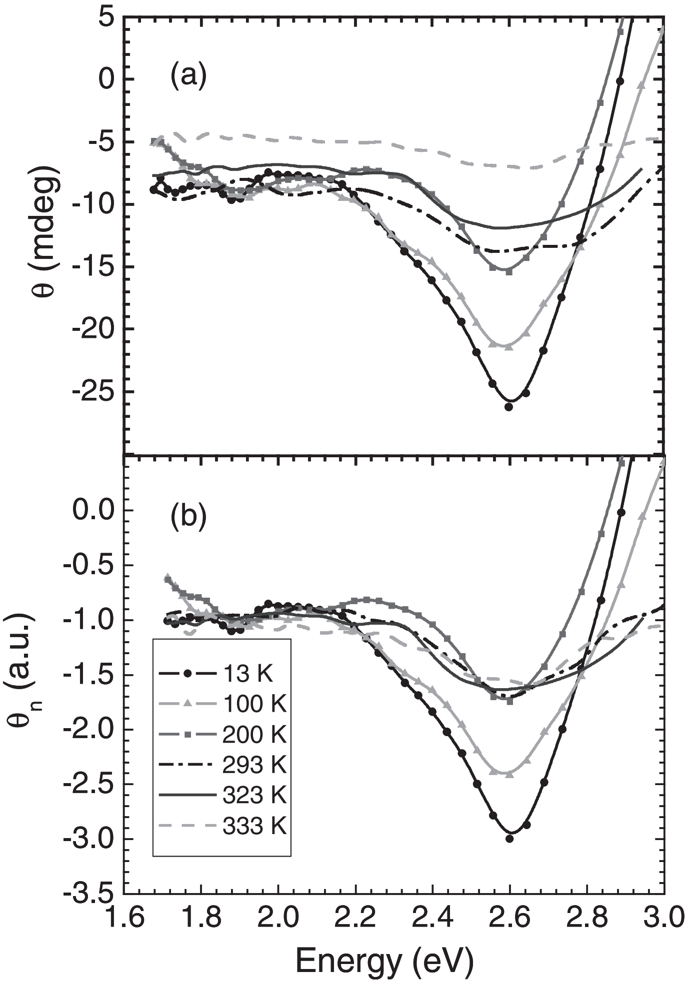

Figure 4. Reflection MCD spectra of an $In_{0.964}Mn_{0.026}As$ thin film, measured with $H = \pm 0.4\,T$, and T ranging between 13 and 333 K. In the top panel (a), the spectra are not normalized. The bottom panel (b) has all spectra normalized with respect to their respective MCD at 1.95 eV after [40].

T' predicted by equations (4)–(6) will be less than the actual concentration. Conversely, the predicted values for S will be greater than the actual concentration of singly substituted Mn.

To determine the role of disorder, a series of MCD spectra for an $In_{0.974}Mn_{0.026}As$ sample was measured between $T = 13$ and 333 K and is shown in figure 4. The spectra are comprised of a broad negative transition from 1.6 to 3.0 eV and a negative peak centered between 2.68 and 2.80 eV. In order to verify that the broad negative background and negative peak are due to two distinct transitions, the MCD spectra at various temperatures were measured and then normalized with respect to their respective values at 1.95 eV. In the case that a dichroism spectrum is composed of two distinct transitions, the MCD at each photon energy would have unique temperature dependence. This also implies that if the dichroism spectra measured at different temperatures are normalized by the MCD at a given photon energy, the spectra would differ. The results following normalization are given in figure 4. For $T > 150$ K, the MCD spectra scale, whereas the 100 and 13 K spectra do not. In fact, figure 4 demonstrates that the negative peak is significantly enhanced with decreasing temperature relative to the broad

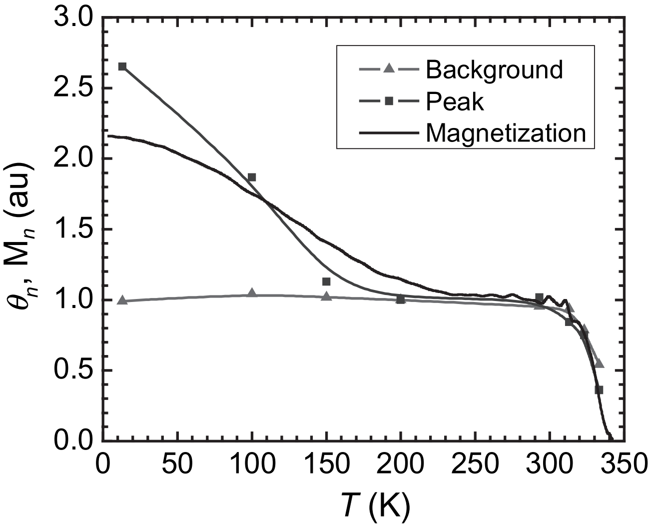

Figure 5. Plot of the MCD at 1.95 and 2.73 eV and M as a function of T for the $\mathrm{In}_{0.964}\mathrm{Mn}_{0.026}\mathrm{As}$ sample. The MCD and M are all normalized with respect to their values at $T = 298$ K after [40].

transition. The magnitudes of the two spectral components and the magnetization as measured by SQUID are plotted as a function of T in figure 5. For comparison, the magnitudes are normalized with respect to their values at 298 K. As seen in figure 5, the temperature dependence of the MCD for the 2.7 eV transition, the background transition and M are similar to one another for temperatures between 200 and 333 K. However, the negative peak increases by a factor 2.7 from $T = 150$ to 13 K. The increase in the peak MCD coincides with the low temperature increase in the magnetization. In contrast, the broad transition response remains relatively constant over the same temperature range.

Several conclusions may be drawn from the temperature dependence of the MCD. First, the significant differences between the temperature dependences of the two MCD spectral features for $T < 150$ K support our previous finding that they involve two different transitions. The spectral response of the MCD (θ) can be described in terms of a superposition of the two transitions as given by the following equation:

$$\theta = -\frac{45}{\pi}\left[\frac{1}{R_{\mathrm{cb-vb}}}\frac{\mathrm{d}R_{\mathrm{cb-vb}}}{\mathrm{d}E}\Delta E_{\mathrm{sp-d}} + \frac{1}{R_{\mathrm{ib-cb}}}\frac{\mathrm{d}R_{\mathrm{ib-cb}}}{\mathrm{d}E}\Delta E_{\mathrm{ib}}\right], \tag{7}$$

whereby the two terms on the right-hand side of equation (7) refer to transitions between the valence and conduction bands (negative peak), and the impurity band to conduction band transitions (broad negative transition), respectively. $R_{\mathrm{cb-vb}}$ is the reflectivity due to valence band to conduction band transitions, which dominates the total reflectivity of the material. $R_{\mathrm{ib-cb}}$ and ΔE_{ib} are the reflectivity due to impurity band to conduction band transitions and its exchange splitting, respectively. We attribute the differences in the temperature dependence of the negative peak and background features to differences in the measured exchange interaction terms for the different optical transitions, that is, $\Delta E_{\mathrm{sp-d}}(T) \neq \Delta E_{\mathrm{ib}}(T)$ [44]. This is in contrast to MBE-grown InMnAs, CdMnTe and ZnCrTe magnetic semiconductors where the dichroism spectrum is only composed of transitions between sp–d exchange split valence and conduction bands (the first term in equation (7)).

As seen in figure 5, the magnitudes of the magnetization and MCD peak at 2.7 eV have a similar temperature dependence at low temperatures. The increase of the absolute peak intensity with temperature implies an enhancement of the sp–d exchange splitting of the valence and conduction bands from equation (7). Therefore, we ascribe the increase in the magnetization at low temperatures to an increase in sp–d exchange coupling. This is consistent with the mean field theory in that the magnetization in a ferromagnetic semiconductor scales with the magnitude of the sp–d exchange constant [44].

Finally, we turn to the temperature dependence of the broad transition to determine the ionization state of Mn at cryogenic temperatures. The negative background has been previously attributed to excitation of electrons from the ionized Mn acceptor impurity (Mn^{2+}) to the conduction band (see equation (2)). At low temperatures whereby $k_\mathrm{B}T \ll E_\mathrm{a}$, where E_a is the ionization energy, the temperature is insufficient to ionize the Mn acceptor, resulting in a low concentration of Mn^{2+} impurities. However, for $k_\mathrm{B}T \ll E_\mathrm{a}$, it is unclear whether the unionized acceptor forms an $\mathrm{Mn}^{2+}+h$ electronic state (where the hole is localized) or an Mn^{3+} state. For an Mn^{3+} state, a decrease in the magnitude of the broad transition would be predicted at cryogenic temperatures. In the case of MOVPE InMnAs, samples with the minimum ionization energy of 3 meV exhibit a significant decrease in the number of holes in the valence band for $T < 50\,\mathrm{K}$ and therefore the number of ionized Mn^{2+} states. However, as seen in figures 4 and 5, the magnitude of the broad transition remains nearly temperature-independent down to $T = 13\,\mathrm{K}$. Therefore, the low temperature MCD implies that Mn is in an $\mathrm{Mn}^{2+}+h$ electronic configuration for $k_\mathrm{B}T \ll E_\mathrm{a}$. This result is consistent with low temperature XMCD measurements of MOVPE InMnAs where $\mathrm{Mn}^{2+}+h$ electronic configuration was also observed at low temperatures.

To determine the nature of the ferromagnetic species that results in the room temperature MCD, we studied the compositional dependence of the dichroism. The MCD spectra of five $\mathrm{In}_{1-x}\mathrm{Mn}_x\mathrm{As}$ samples at $T = 298\,\mathrm{K}$ are plotted in figure 6. Since the response above 2.2 eV consists of the superposition of two transitions, in figure 6 the contribution of the broad transition response was subtracted from the total response to determine the dependence of the magnitude of the negative peak on Mn concentration. As seen in figure 6 the most significant aspect of the MCD is a superlinear increase in the magnitudes of both transitions with x.

The magnitudes of the background ($|\theta_\mathrm{b}|$) and peak ($|\theta_\mathrm{p}|$) dichroism were measured at 1.95 and 2.73 eV from figure 6. The plots of $|\theta_\mathrm{b}|$ and $|\theta_\mathrm{p}|$ as a function of x are given in figures 7(a) and (b), respectively. The magnitude of the term $\frac{1}{R_{\mathrm{vb-cb}}}\frac{\mathrm{d}R_{\mathrm{vb-cb}}}{\mathrm{d}E}(2.73\,\mathrm{eV})$ is 0.12 and was determined from earlier reflectivity measurements of InMnAs. A similar procedure was not used to determine ΔE_{ib}, because $R_{\mathrm{ib-cb}}$ cannot be independently measured. Inspection of the experimental data in figure 7 indicates that the MCD response of the background and peak are superlinear in x. The deviations from linearity are particularly apparent at high Mn concentrations. The superlinearity is a signature of cluster formation which would be expected for high concentration alloys especially if the thermodynamics of cluster formation are favorable. In this case the clusters consist of substitutional Mn on nearest neighbor cation sites.

The composition dependence of $|\theta_\mathrm{b}|$ and $|\theta_\mathrm{p}|$ as a function of x shown in figures 7(a) and (b) was fitted with respect to four different cluster configurations. The fitting assumes that the dichroism is proportional to the concentration of the four specific cluster species in the material. However, we emphasize that a nonzero binding energy would not affect the *lineshape* of the cluster concentration versus x plot. For example, Reiss *et al* [36] demonstrated that the concentration of dimers has an x^2 dependence, regardless of the magnitude of the binding

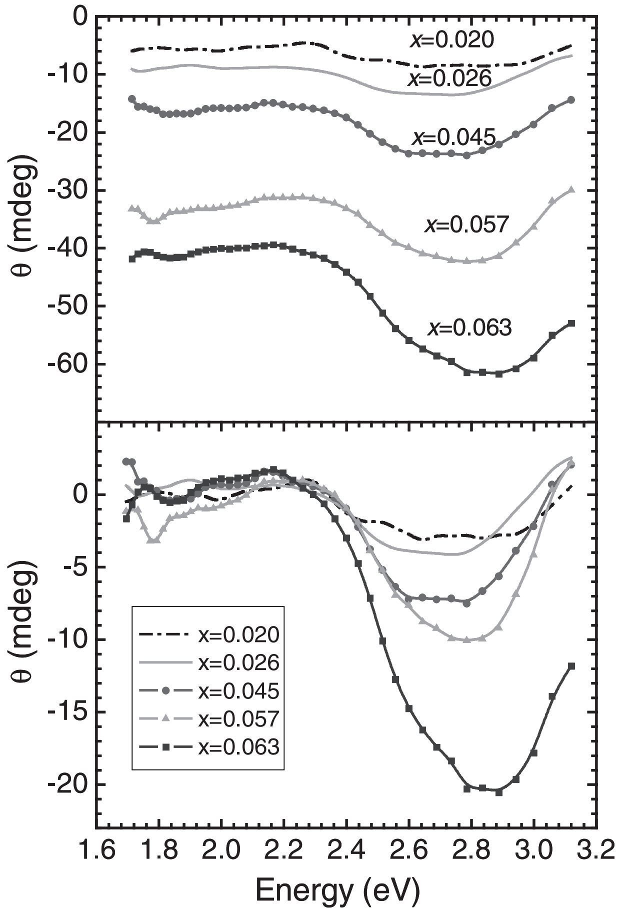

Figure 6. Reflection MCD spectra of five $In_{1-x}Mn_xAs$ samples with x ranging between 0.020 and 0.063 (a) including the broad transition, (b) with the background subtracted. All spectra were measured at room temperature with an applied field of 0.4 T after [40].

energy. Therefore, the fits of the dichroism and its composition dependence using the previous expressions for S, D, T and T' will still be valid since binding energies do not affect the shape of the θ versus x plots.

Plots of the measured $|\theta_b|$ and $|\theta_p|$ versus x dependence and the corresponding fits using equations (3)–(6) are shown in figures 7(a) and (b), respectively. A_n was used as a fitting parameter. As shown in figures 7(a) and (b), the agreement of the experimental composition dependence with the cluster model improves with increasing cluster size, n. In particular, the model that attributes the dichroism to tetramers ($n = 4$) reproduces the superlinear dependence of both $|\theta_b|$ and $|\theta_p|$ on x at high Mn concentrations. In contrast, the calculation that attributes the dichroism to singly substituted Mn significantly underestimates the magnitude of the dichroism at high Mn concentrations. Improvement of the fit of the composition dependence with increasing cluster size is also evident from the R^2 values. The singly substituted Mn model fit of $|\theta_b|$ versus x has an R^2 value of 0.63. The R^2 values increase to 0.89 for the dimer model fit and to 0.97 for the trimer model fit. The fit with the highest R^2 value corresponds to the tetramer configuration (0.99). A similar improvement in R^2 values from 0.60 to 0.92 with increasing

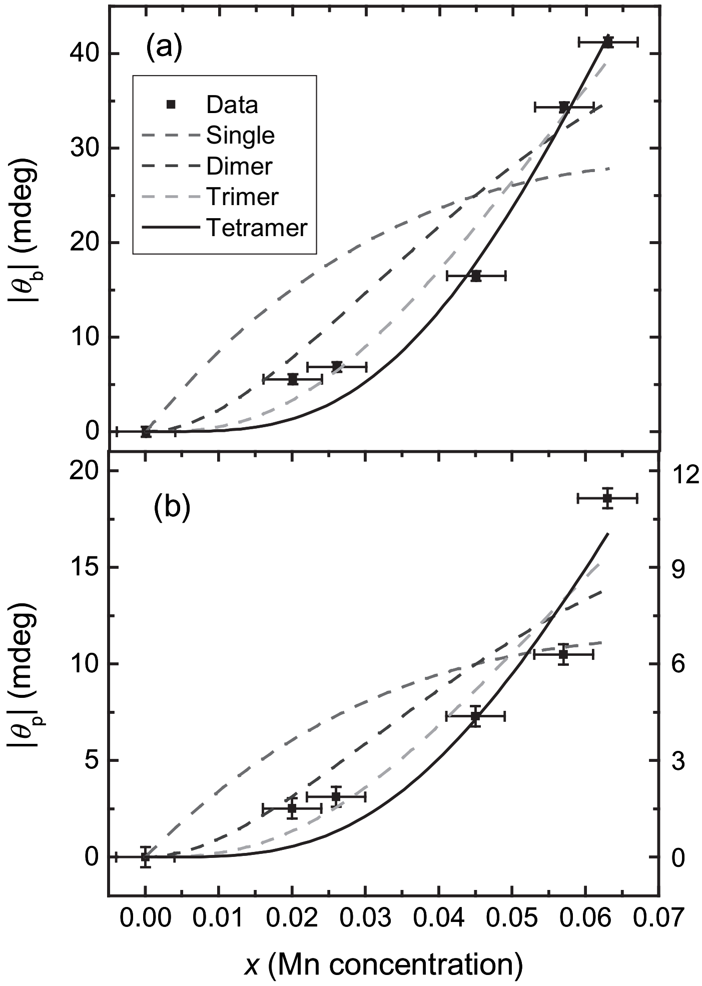

Figure 7. Dependence of (a) $|\theta_b|(1.95\,\mathrm{eV})$, (b) $|\theta_p|(2.73\,\mathrm{eV})$ and $\Delta E_{\mathrm{sp-d}}(2.73\,\mathrm{eV})$ on x. The dotted and solid lines correspond to linear and pair model fits, respectively, after [40].

cluster size was observed in the fits of the $|\theta_p|$ versus x dependence. Therefore, the excellent agreement of the compositional dependence of the MCD with the cluster model suggests that both the broad transition and negative peak are related to Mn clusters, a result consistent with our earlier EXAFS work [38].

The cluster model for the compositional dependence of the MCD suggests that the Mn-related electronic states that give rise to the broad background are also associated with clusters. It is Mn 3d states within the cluster that form the impurity band. Furthermore, these 3d states in the impurity band couple with the states in the valence and conduction bands. The exchange between the 3d states of the *Mn clusters* with semiconductor host states results in a large sp–d exchange splitting that persists past room temperature. In contrast, hybridization of singly substituted Mn 3d states (i.e. MBE InMnAs) results in a weaker sp–d exchange splitting that is limited to 90 K. The presence of these Mn cluster states is necessary for sp–d exchange splitting of the valence and conduction bands to persist up to room temperature.

These findings based upon MCD measurements are supported by first principles calculations of disordered ferromagnetic semiconductors by Raebiger *et al* [45] using the projector augmented-wave method. They predicted that well-defined electronic states form in the band gap from Mn clusters with sizes ranging from $n = 1$ to 5. The same Mn 3d cluster states hybridize with valence and conduction bands sp band states. The calculation also predicted an increase in the strength of sp–d exchange with increased Mn clustering.

To summarize the magneto-optical measurements, spectrally resolved MCD of InMnAs was measured over the energy range of 1.6–3.0 eV. A strong dependence of the magnitude of the negative peak MCD associated with sp–d exchange was observed that corresponds to a low temperature increase in the SQUID magnetization. In contrast, the broad transition ascribed to impurity band to conduction band transitions is nearly temperature-independent for temperatures below 150 K. The superlinear compositional dependence of the two MCD features is attributed to the presence of ferromagnetic Mn atomic clusters. These clusters play a critical role in the stabilization of ferromagnetism in these alloys.

4. Summary and outlook

In this paper, we report on the role of short-range disorder in stabilizing ferromagnetism in transition metal-doped semiconductors. While both prior theory and experiment have centered on DMSs where the magnetic ions substitute randomly on cation sites, there is growing evidence that correlated substitution needs to be considered. Evidence of correlated substitution comes from structural analysis (EXAFS), magnetic property and magneto-optical property measurements as well as theory. Furthermore, there is growing theoretical and experimental evidence that non-random substitution can result in ferromagnetic semiconductors with Curie temperatures well above room temperature. Future materials research will be well served by identification and examination of semiconductor systems that favor short-range ordering of magnetic constituents.

Acknowledgments

I thank A Blattner and P T Chiu of the Electronic and Photonic Materials group at Northwestern for their contributions throughout this work. The work at Northwestern University was supported by a grant from the NSF (DMR-0511523).

References

[1] Ohno H 1998 Making nonmagnetic semiconductors ferromagnetic *Science* **281** 951
[2] Akinaga H and Ohno H 2002 Semiconductor spintronics *IEEE Trans. Nanotechnol.* **1** 19–31
[3] Furdyna J K 1982 Diluted magnetic semiconductors—an interface of semiconductor physics and magnetism *J. Appl. Phys.* **53** 637
[4] Munekata H, Ohno H, von Molnar S, Segmuller A, Chang L L and Esaki L 1989 Diluted magnetic III–V semiconductors *Phys. Rev. Lett.* **63** 1849
[5] Ohno H *et al* 1996 GaMnAs, a new diluted magnetic semiconductor based on GaAs *Appl. Phys. Lett.* **69** 363
[6] Dietl T, Ohno H, Matsukura F, Cibert J and Ferrand D 2000 Zener model description of ferromagnetism in zinc-blende magnetic semiconductors *Science* **287** 1019

[7] Larson B E, Hass K C, Ehrenreich H and Carlson A E 1988 Theory of exchange interactions and chemical trends in diluted magnetic semiconductors *Phys. Rev.* B **37** 4137

[8] Dietl T, Ohno H and Matsukura F 2001 Hole-mediated ferromagnetism in tetrahedrally coordinated semiconductors *Phys. Rev.* B **63** 195205

[9] Schallenberg T and Munekata H 2006 Preparation of ferromagnetic InMnAs with a high Curie temperature of 90 K *Appl. Phys. Lett.* **89** 042507

[10] Bouzerear R, Bouzerar G and Ziman T 2006 Why RKKY exchange integrals are inappropriate to describe ferromagnetism in diluted magnetic semiconductors *Phys. Rev.* B **73** 024411

[11] Bouzerar G, Ziman T and Kudrnovsky J 2005 Calculating the Curie temperature reliably in diluted III–V ferromagnetic semiconductors *Europhys. Lett.* **69** 812

[12] Bergvist L *et al* 2004 Magnetic percolation in diluted magnetic semiconductors *Phys. Rev.* B **93** 137202

[13] Sato K, Schweika W, Dederichs P H and Katayama-Yoshida H 2004 Low-temperature ferromagnetism in (Ga,Mn)N: *ab initio* calculations *Phys. Rev.* B **70** 201202

[14] Bouzerar G, Ziman T and Kudrnovsky J 2004 Can correlated substitution enhance the Curie temperature in diluted magnetic semiconductors? *Appl. Phys. Lett.* **85** 4941–3

[15] Blattner A J, Lensch J and Wessels B W 2001 Growth and characterization of OMVPE grown (In, Mn)As diluted magnetic semiconductor *J. Electron. Mater.* **30** 1408

[16] Blattner A J and Wessels B W 2002 Ferromagnetism in (In, Mn)As diluted magnetic semiconductor thin films grown by metalorganic vapor phase epitaxy *J. Vac. Sci. Technol.* B **20** 1582

[17] Blattner A J, Prabhumirahi P L, Dravid V and Wessels B W 2003 Origin of room temperature ferromagnetism in homogeneous (In,MnAs) *J. Cryst. Growth* **259** 8

[18] Blattner A J and Wessels B W 2004 Ferromagnetism in (In, Mn)As alloy thin films *Appl. Surf. Sci.* **221** 155

[19] Grandidier B *et al* 2000 Atomic-scale study of GaMnAs/GaAs layers *Appl. Phys. Lett.* **77** 4001

[20] Yu K M *et al* 2003 Curie temperature limit in ferromagnetic GaMnAs *Phys. Rev.* B **68** 041308

[21] Burns G 1985 *Solid State Physics* (New York: Academic)

[22] Coey J M D 2006 Dilute magnetic oxides *Curr. Opin. Solid State Mater. Sci.* **10** 83

[23] Mahadevan P and Zunger A 2004 Trends in ferromagnetism, hole localization and acceptor level depth for Mn substitution in GaN, GaP, GaAs and GaSb *Appl. Phys. Lett.* **85** 2860

[24] Korotkov R, Gregie J M and Wessels B W 2002 Optical properties of deep Mn acceptor in GaN *Appl. Phys. Lett.* **80** 1731

[25] Huang K and Wessels B W 1988 Characterization of Mn-doped InAsP grown by organometallic vapor phase epitaxy *Appl. Phys. Lett.* **52** 1155

[26] Kudnrovsky J, Drchal V, Bouzerar G and Bouzerar R 2007 Ordering effects in diluted magnetic semiconductors *Phase Transit.* **80** 333–50

[27] Sato K, Katayama-Yoshida H and Dederichs P H 2005 High Curie temperature and nano-scale spinodal decomposition phase in dilute magnetic semiconductors *Japan J. Appl. Phys.* **44** L948

[28] Kuruda S *et al* 2007 Origin and control of high temperature ferromagnetism in semiconductors *Nat. Mater.* **6** 440–6

[29] Samarth N 2007 Ruled by a magnetic-rich minority phase *Nat. Mater.* **6** 403

[30] Fukushima T, Sato K, Katayama-Yoshida H and Dederichs P H 2006 Spinodal decomposition under layer by layer growth and high Curie temperature quasi-one dimensional nano-structure in dilute magnetic semiconductors *Japan J. Appl. Phys.* **45** L416

[31] Katayama-Yoshida H *et al* 2007 Computational nano-materials design for high T_c ferromagnetism in wide-gap magnetic semiconductors *J. Magn. Magn. Mater.* **310** 2070

[32] Sato K, Fukushima T and Katayama-Yoshida H 2007 Super-paramagnetic blocking phenomena and room-temperature ferromagnetism in wide band-gap dilute magnetic semiconductor (Ga,Mn)N *Japan J. Appl. Phys.* **46** L682

[33] Franceschetti A *et al* 2006 First principles combinatorial design of transition temperatures in multicomponent systems: the case of Mn in GaAs *Phys. Rev. Lett.* **97** 047202

[34] Blattner A J, Prabhumirahi P L, Dravid V and Wessels B W 2003 Origin of room temperature ferromagnetism in homogeneous (In,MnAs) *J. Cryst. Growth* **259** 8

[35] May S J 2007 *PhD Thesis* Northwestern University.

[36] Reiss H, Fuller C S and Morin F J 1956 Chemical interactions among defects in germanium and silicon *Bell Syst. Tech. J.* **35** 535

[37] Blattner A J 2004 *PhD Thesis* Northwestern University

[38] Soo Y *et al* 2004 Local structure around Mn atoms in room temperature ferromagnetic (In,Mn)As thin films probed by extended x-ray absorption fine structure *Appl. Phys. Lett.* **84** 481

[39] Soo Y L *et al* 1996 III–V diluted magnetic semiconductor: substitutional doping of Mn in InAs *Phys. Rev.* B **53** 4905

[40] Chiu P T and Wessels B W 2006 Dependence of magnetic circular dichroism on doping and temperature in InMnAs epitaxial films *Phys. Rev.* B **76** 165201

[41] Ando K 2006 Seeking room-temperature ferromagnetic semiconductors *Science* **312** 1883

[42] Chiu P T, Wessels B W, Keavney D J and Freeland J W 2005 Local environment of ferromagnetically ordered Mn in epitaxial InMnAs *Appl. Phys. Lett.* **86** 072505

[43] Behringer R E 1958 Number of single, double and triple clusters in a system containing 2 types of clusters *J. Chem. Phys.* **29** 537

[44] Ando K 2000 *Magneto-optics* (Berlin: Springer)

[45] Raebinger H, Ayuela A and von Boehm J 2005 Electronic and magnetic properties of substitutional Mn clusters in (Ga,Mn)As *Phys. Rev.* B **72** 014465